JOURNAL OF Applied Polymer SCIENCE

Response Surface Predictions of the Viscoelastic Properties of Vapor-Grown Carbon Nanofiber/Vinyl Ester Nanocomposites

Sasan Nouranian,[1,2] Thomas E. Lacy,[3] Hossein Toghiani,[1] Charles U. Pittman Jr.,[4] Janice L. DuBien[5]

[1]The Dave C. Swalm School of Chemical Engineering, Mississippi State University, Mississippi State, Mississippi 39762
[2]Center for Advanced Vehicular Systems (CAVS), Mississippi State, Mississippi 39762-5405
[3]Department of Aerospace Engineering, Mississippi State University, Mississippi State, Mississippi 39762
[4]Department of Chemistry, Mississippi State University, Mississippi State, Mississippi 39762
[5]Department of Mathematics and Statistics, Mississippi State University, Mississippi State, Mississippi 39762
Correspondence to: H. Toghiani (E-mail: hossein@che.msstate.edu)

ABSTRACT: A full factorial design of experiments and response surface methodology were used to investigate the effects of formulation, processing, and operating temperature on the viscoelastic properties of vapor-grown carbon nanofiber (VGCNF)/vinyl ester (VE) nanocomposites. Factors included VGCNF type (pristine, oxidized), use of a dispersing agent (DA) (no, yes), mixing method (ultrasonication, high-shear mixing, and a combination of both), VGCNF weight fraction (0.00, 0.25, 0.50, 0.75, and 1.00 parts per hundred parts resin (phr)), and temperature (30, 60, 90, and 120°C). Response surface models (RSMs) for predicting storage and loss moduli were developed, which explicitly account for the effect of complex interactions between nanocomposite design factors and operating temperature on resultant composite properties; such influences would be impossible to assess using traditional single-factor experiments. Nanocomposite storage moduli were maximized over the entire temperature range (~20% increase over neat VE) by using high-shear mixing and oxidized VGCNFs with DA or equivalently by employing pristine VGCNFs without DA at ~0.40 phr of VGCNFs. Ultrasonication yielded the highest loss modulus at ~0.25 phr of VGCNFs. The RSMs developed in this investigation may be used to design VGCNF-enhanced VE matrices with optimal storage and loss moduli for automotive structural applications. Moreover, a similar approach may be used to tailor the mechanical, thermal, and electrical properties of nanomaterials over a range of anticipated operating environments. © 2013 Wiley Periodicals, Inc. J. Appl. Polym. Sci. 130: 234–247, 2013

KEYWORDS: composites; mechanical properties; thermosets

Received 30 July 2012; accepted 20 January 2013; published online 14 March 2013
DOI: 10.1002/app.39041

INTRODUCTION

Polymer nanocomposites have promising physical and mechanical performance in many applications.[1–3] In the automotive and aerospace industries, thermoset polymer nanocomposites are attracting increased attention as their exceptional multifunctional properties are discovered.[4] Carbon nanotubes, carbon nanofibers, graphene platelets, silica nanoparticles, and nanoclays are often used as nanoreinforcements in these materials.[5] Recently, vapor-grown carbon nanofibers (VGCNFs) have been used to reinforce a variety of polymer matrices.[6]

Successful attempts have been made to improve composite properties such as thermal conductivity,[7–10] dielectric properties,[11] electrical conductivity,[8,12–14] electromagnetic interference shielding,[15–17] and flame retardancy[18] by incorporation of VGCNFs in the matrix. However, composite mechanical property improvements have largely been compromised by poor nanofiber dispersion in the matrix, inadequate nanofiber alignment, and weak nanofiber-matrix interfacial adhesion.[6] Different attempts have been made to improve nanofiber dispersion through surface functionalization,[19–21] use of a dispersing agent,[22] or utilizing different mixing methods.[23–26] However, such studies have largely considered the isolated effect of only one fabrication/processing factor. Hence, the results obtained using a *one-at-a-time* (single factor) experimental approach explicitly neglect the complex interactions between factors. Optimal nanocomposite fabrication requires the use of a systematic statistical approach, such as design of experiments[27] and response surface methodology,[28] to understand the interactions between different formulation, processing, and other factors and their effects on material properties. The significance of using design of experiments and response surface modeling in composite materials research has received increased recognition.[29] For example, such statistical methods have been used in the

design, mechanical characterization, and optimization of sandwich composites,[30–32] polymers, and polymer nanocomposites.[33–38]

VGCNF/vinyl ester (VE) nanocomposites are promising materials for use as nanoenhanced and/or multifunctional matrices in continuous fiber or laminated composite structures because of their enhanced material properties in comparison to matrices composed of neat VE. For example, the matrix can be stiffened by VGCNF addition without generating a higher crosslink density. Their tensile, flexural,[39] impact,[40] and high-strain-rate behavior[41] have been studied. The effects of four formulation and processing factors (VGCNF type, the use of a dispersing agent, mixing method, and VGCNF weight fraction) on *room temperature* storage and loss moduli of VGCNF/VE nanocomposites were previously investigated by the authors using design of experiments and response surface modeling.[42] Thermal behavior may also be characterized and optimized to provide a more comprehensive design, since the temperature-dependent material response plays a crucial role during in-service performance. Nanoreinforcements may significantly affect the thermomechanical behavior of the cured nanophased matrix, including its glass transition temperature (T_g) and thermal expansion behavior.[43–47]

Polymer viscoelastic behavior is efficiently studied using dynamic mechanical analysis (DMA).[48] In this technique, a complex modulus comprised of a real elastic part (storage modulus) and an imaginary energy dissipative part (loss modulus) is measured. The storage modulus is proportional to the Young's modulus of the material. The loss modulus is one indicator of a material's energy absorption capability. This capability together with material's damping characteristics is utilized for reducing vibration and/or noise in heavy machinery, aircraft, and other vehicle applications.[49] An automotive structure needs to possess both high stiffness and high energy absorption capability to ensure structural rigidity and crashworthiness. Apart from loss modulus, impact strength, impact toughness, fracture toughness, strain energy release rate, and ductility have also been associated with changes in material's energy absorption characteristics.[50]

In the current study, a robust statistical design of experiments approach is employed to investigate the coupled effects of formulation and processing factors and operating temperature on the viscoelastic properties of VGCNF/VE nanocomposites. Response surface models (RSMs) are developed for predicting nanocomposite storage and loss moduli as a function of VGCNF type, the use of a dispersing agent, mixing method, VGCNF weight fraction, and operating temperature. The inclusion of temperature as an additional independent variable represents a substantial increase in the experimental design space from our previous study.[42] Modest changes in operating temperature consistent with typical automotive applications can have a profound effect on the viscoelastic response of polymer nanocomposites; this is of critical importance when assessing time-dependent material behavior and crashworthiness at elevated temperatures. The RSMs developed in this investigation may be used to design VGCNF-enhanced VE matrices with optimal storage and loss moduli for automotive structural applications. More generally, response surface methodologies may readily be used to tailor the mechanical, thermal, and electrical properties of multifunctional nanocomposites over a range of anticipated operating environments.

EXPERIMENTAL

Statistical Experimental Design

A general mixed-level full factorial design was utilized to systematically investigate and model the effects of three qualitative and two quantitative factors on the VGCNF/VE nanocomposite storage and loss moduli. The factors and their levels were selected to address two critical aspects of nanocomposite fabrication, i.e., nanofiber dispersion and nanofiber-matrix interfacial adhesion. Since the current study represents an extension of the work performed by Nouranian et al.[42] no screening experiments were conducted . The qualitative factors included the VGCNF type (designated as *A*) in two levels (pristine, oxidized), the use of dispersing agent (*B*) in two levels (no, yes), and the mixing method (*C*) in three levels (ultrasonication, high-shear mixing, and a combination of both). Moreover, the two quantitative factors were VGCNF weight fraction (*W*) in five levels (0.00, 0.25, 0.50, 0.75, and 1.00 parts per hundred parts resin (phr)) and temperature (*T*) in four levels (30, 60, 90, and 120°C). One long-term objective was to ensure that the viscosity of the nanoreinforced resin remained relatively low in order to permit future resin infusion into continuous fiber preforms. VGCNF weight fractions in excess of 1.00 phr can lead to VGCNF/VE blends with a paste-like consistency and were not considered here. All samples used the same starting resin and curing protocol. An elevated curing temperature was employed to enhance the overall reaction rate, increase diffusion within the crosslinking matrix, and facilitate specimen preparation times. The current curing protocol was based upon recommendations by the resin manufacturer. The experimental design factors and their respective levels are shown in Table I. The temperature levels were selected in equally spaced intervals ranging from 30°C to 120°C, all below the material's glass transition temperature. Storage and loss moduli were selected as the responses of interest. Data analyses were performed using the SAS® V9.2 statistical analysis software.

Nanocomposite Materials and Dynamic Mechanical Analysis

A commercial, 33 wt % styrene, liquid VE resin (Derakane 441-400, Ashland, Covington, KY) was employed for the matrix. It was cured by free radical addition polymerization using methyl ethyl ketone peroxide (MEKP) (US Composites) as the initiator. A 6% solution of cobalt naphthenate (North American Composites) promoter was used to accelerate MEKP decomposition. Two commercial air release additives, BYK-A515 and BYK-A555 (BYK Chemie, GmbH), were employed to remove air bubbles that were introduced during mixing of the viscous VGCNF/VE blend. The pristine and oxidized VGCNFs (PR24-XT-LHT and PR24-XT-LHT-OX, respectively, both from Applied Sciences) were used as carbon nanofibers of choice. Nanofiber surface oxidation is commonly employed to improve the interfacial adhesion between the nanofibers and the matrix.[21] Specimens were

Table I. Factors Used in This Study and Their Levels

Factor designation	Factor	Levels				
		1	2	3	4	5
A	VGCNF[a] type	Pristine	Oxidized	-	-	-
B	Use of dispersing agent	No	Yes	-	-	-
C	Mixing method	US[b]	HS[c]	HS/US[d]	-	-
W	VGCNF weight fraction (phr[e])	0	0.25	0.50	0.75	1.00
T	Temperature (°C)	30	60	90	120	-

[a]Vapor-grown carbon nanofiber, [b]Ultrasonic mixing, [c]High-shear mixing, [d]Combined high-shear and ultrasonic mixing, [e]Parts per hundred parts resin.

Table II. Nanocomposite Formulations Based on the Experimental Design

Ingredient	Weight (g)
Derakane 441-400	100
Cobalt naphthenate 6%	0.20
BYK-A 515	0.20
BYK-A 555	0.20
BYK-9076[a]	1 : 1 ratio with respect to VGCNF
VGCNF (pristine or oxidized)	0.00/0.25/0.50/0.75/1.00
MEKP	1.00

Note: all ingredients were used in fixed amounts, except for the dispersing agent and the VGCNFs. These components were added in amounts directed by the design.
[a]The dispersing agent was added in an amount directly proportional to the VGCNF weight.

prepared using the general formulation outlined in Table II, where the amounts of VGCNFs and dispersing agent, BYK-9076 (BYK Chemie, GmbH), were employed at the particular factor level combinations dictated by the experimental design. The ratio of the dispersing agent amount to the amount of VGCNFs was 1 : 1 by weight to maximize its efficiency. Test specimens were prepared according to the protocol described previously.[42] A schematic of this protocol is given in Figure 1.

Three separate nanocomposite specimens were prepared for each treatment combination (combination of various factor levels). Specimens were polished before testing and the final average dimensions were 17.5 × 12.5 × 3.5 mm^3. Nanocomposite storage and loss moduli were measured as a function of temperature with a Dynamic Mechanical Analyzer in a single cantilever mode at an amplitude of 15 μm.[42] The frequency (10 Hz) and a heating rate (5 C/min) were held fixed and storage and loss moduli were measured over a temperature range of 27–160°C. While a frequency of 1 Hz is often employed for the DMA test of a polymer specimen under a temperature sweep, we were motivated to use 10 Hz based on previous work by Li et al.[51] on nanoreinforced epoxy composites.

RESULTS AND DISCUSSION

The average storage and loss moduli for each treatment combination (run) for a total of 240 (2 × 2 × 3 × 5 × 4) treatment combinations are given by Nouranian.[52] The storage

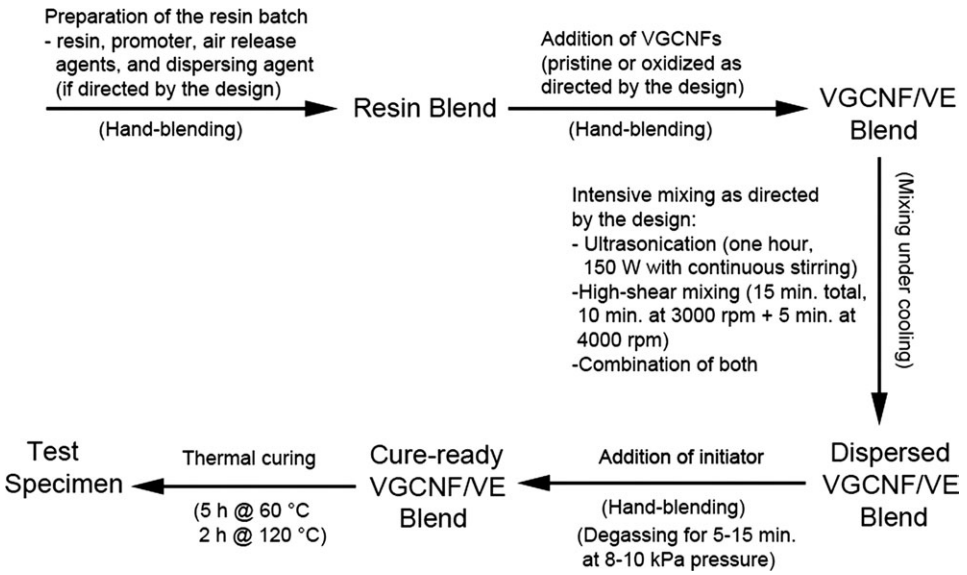

Figure 1. Schematic of the specimen preparation protocol.

Table III. Analysis of Variance (ANOVA) for the Storage Modulus Data

Source of variation	Degrees of freedom	Sum of squares	Mean square	*F*-Value	*P*-Value[a]
Model	141	81807482.4	580194.9	126.3	<0.0001
A: VGCNF type	1	28427.3	28427.3	6.2	0.0146
B: Use of dispersing agent	1	49020.4	49020.4	10.7	0.0015
C: Mixing method	2	2466492.2	1233246.1	268.4	<0.0001
W: VGCNF weight fraction	4	6441727.2	1610431.8	350.5	<0.0001
T: Temperature	3	69692014.4	23230671.5	5056.4	<0.0001
A×*B*	1	546.0	546.0	0.1	0.7310
A×*C*	2	46155.8	23077.9	5.0	0.0084
A×*W*	4	35429.2	8857.3	1.9	0.1118
A×*T*	3	21266.7	7088.9	1.5	0.2082
B×*C*	2	137845.4	68922.7	15.0	<0.0001
B×*W*	4	50122.7	12530.7	2.7	0.0335
B×*T*	3	9973.9	3324.6	0.7	0.5402
C×*W*	8	694447.1	86805.9	18.9	<0.0001
C×*T*	6	767507.3	127917.9	27.8	<0.0001
W×*T*	12	426069.7	35505.8	7.7	<0.0001
A×*B*×*C*	2	114141.0	57070.5	12.4	<0.0001
A×*B*×*W*	4	74059.2	18514.8	4.0	0.0046
A×*B*×*T*	3	6214.9	2071.6	0.5	0.7172
A×*C*×*W*	8	40655.1	5081.9	1.1	0.3658
A×*C*×*T*	6	26980.3	4496.7	1.0	0.4438
A×*W*×*T*	12	46375.1	3864.6	0.8	0.6083
B×*C*×*W*	8	256564.4	32070.6	7.0	<0.0001
B×*C*×*T*	6	78605.2	13100.9	2.9	0.0133
B×*W*×*T*	12	12397.4	1033.1	0.2	0.9968
C×*W*×*T*	24	284444.4	11851.9	2.6	0.0006
Error	98	450246.0	4594.4	-	-
Total (corrected)	239	82257728.4	-	-	-
Other Model Statistics					
Mean: 1929.2			R^2: 0.995		
Coefficient of variation: 3.5%			Standard deviation: 67.8		

Note: The underlined three-factor interactions are significant. The lower order significant interactions were not considered in the analysis, because they are all contained in higher order interactions.
[a]Values less than 0.05 are considered significant in the analysis.

moduli fell in the range $S = 550$–2766 MPa with an average standard deviation of 50–100 MPa. The loss moduli were in the range $L = 41$–208 MPa with an average standard deviation of 5–10 MPa. The treatment combination responses for different temperatures at fixed levels of the other factors were all collected from the experimental data obtained for the storage and loss moduli as a function of temperature in the range of 27–160°C. Forty-eight treatment combinations with a VGCNF weight fraction of 0.00 phr belonged to the neat VE. These had all the same response values regardless of other factor levels. For example, the VGCNF type and mixing method are irrelevant at 0.00 phr VGCNF and no dispersing agent is used in the neat resin formulation. Therefore, only 49 actual DMA measurements were performed for the 240 treatment combinations. The neat VE was considered as part of the design and not as a control factor since it was of critical interest to capture the neat VE's behavior in the RSMs.

Storage Moduli

Storage modulus data were first subjected to the analysis of variance (ANOVA) method[27] before predictive RSMs were developed. Since there was only one run per treatment combination (i.e., only one batch of the material was prepared based on the dictated factor level combinations) no measure of pure (experimental) error was obtained. Therefore, four- and five-factor interactions (the two highest order interactions) were assumed to be negligible to construct an error term for the ANOVA. The ANOVA results are shown in Table III, where the main, two-, and three-factor interaction effects are

Table IV. Multiple Comparison Results for the Mean Storage Modulus Data Using Least Significant Difference (LSD) for the Interaction Between the VGCNF Type, the Use of Dispersing Agent, and the Mixing Method ($A \times B \times C$)

t-Grouping		Least squares mean values for the storage modulus data (MPa)	VGCNF type (A)	Use of dispersing agent (B)	Mixing method (C)	
	M[a]	2026.2	Oxidized	No	HS[b]	
	M					
N	M	2021.9	Pristine	No	HS/US[c]	
N	M					
N	M	2017.0	Pristine	Yes	HS[d]	
N	M					
N	M	2016.5	Oxidized	No	HS/US	
N	M					S1
N	M	2006.3	Pristine	Yes	HS/US	
N	M					
N	M	1994.2	Oxidized	Yes	HS	
N						
N	O	1980.7	Oxidized	Yes	HS/US	
	O					
	O	1943.9	Pristine	No	HS	
	P	1883.8	Oxidized	Yes	US	S2
	Q	1779.1	Pristine	Yes	US	
	Q					
	Q	1741.8	Pristine	No	US/US	S3
	Q					
	Q	1739.3	Oxidized	No	US	

Each group of data, i.e., S1, S2, and S3, results in one response surface.
[a]Least squares mean values with the same letters are not significantly different from each other.
[b]High-shear mixing.
[c]Combined high-shear and ultrasonic mixing.
[d]High-shear mixing.

displayed. Ordered *F*-tests[53] were conducted on the factorial effects starting from the highest order (three-factor) interactions. The factorial effects with *P*-values less than $\alpha = 0.05$ (5% level of significance) were considered significant for this analysis (Table III). $\alpha = 0.05$ is the standard and common value used for statistical hypothesis tests. On this basis, five three-factor interactions (all underlined in Table III) were considered significant. These included:

1. Interaction between the type of VGCNF (A), the use of dispersing agent (B), and the mixing method (C), i.e., $A \times B \times$C;
2. Interaction between the type of VGCNF (A), the use of dispersing agent (B), and the VGCNF weight fraction (W), i.e., $A \times B \times W$;
3. Interaction between the use of dispersing agent (B), the mixing method (C), and the VGCNF weight fraction (W), i.e., $B \times C \times W$;
4. Interaction between the use of dispersing agent (B), the mixing method (C), and the temperature (T), i.e., $B \times C \times T$;
5. Interaction between the mixing method (C), the VGCNF weight fraction (W), and the temperature (T), i.e., $C \times W \times T$.

Most of the main effects and two-factor interactions in Table III were not "clean," meaning they were completely contained in higher-order significant three-factor interactions. Therefore, they were not further analyzed even when their *P*-values were less than 0.05. The only clean two-factor interaction, the $A \times T$ interaction, was not significant (*P*-value $= 0.2082 > 0.05$). The two quantitative factors, VGCNF weight fraction (W) and temperature (T), were used to generate the RSMs. Twelve different three-dimensional (3D) response surfaces could be generated from *all* combinations of the qualitative factors ($2 \times 2 \times 3 = 12$ combinations, where the numbers in the left-hand side of the equality denote factor levels). These responses would all be continuous functions of VGCNF weight fraction and temperature. However, analysis of the significant $A \times B \times C$ interaction, where all three factors are qualitative, can be used to determine the significant factor combinations out of the 12 total combinations. This permits a reduction of the total

number of generated response surfaces. All of the other significant three-factor interactions involved quantitative factors (i.e., VGCNF weight fraction and temperature). Since these were already considered in the response surfaces, they were not further analyzed.

Fisher's protected least significant difference (LSD) multiple comparisons[28] were conducted at $\alpha = 0.05$ on the mean values associated with the $A \times B \times C$ interaction in order to isolate significant qualitative factor level combinations. These results appear in Table IV, where the mean values associated with each "VGCNF type/dispersing agent/mixing method" combination are compared with the mean values for the other combinations. In the LSD comparisons, an LSD value is calculated[28] and *t*-tests are run on pair-wise differences between the mean values. Calculated *t*-values greater than the LSD value define which differences are significant. These comparisons of the mean values are better represented by a standard graphical format represented in Table IV. When two mean values are compared, only those with different designated letters (M, N, O, P, and Q) in their *t*-grouping column of Table IV are significantly different from each other. The letters in the *t*-grouping column can comprise one, two, or several subcolumns. For example, the combination "pristine nanofibers/no dispersing agent/combination of high-shear mixing and ultrasonication (HS/US)" has letters M and N in its *t*-grouping column. Therefore, its associated mean storage modulus is significantly different from the mean storage modulus for the combination "pristine nanofibers/no dispersing agent/HS," which has only the letter O in its *t*-grouping column. If a single letter was common between the two distinct qualitative factor level combinations, then only an insignificant difference exists in their mean storage moduli. This suggests that a single RSM can be used to represent both factor level combinations.

Following similar arguments, the first eight combinations in Table IV, i.e., HS and HS/US combinations, are "chained" in the *t*-grouping column as evident by the uninterrupted linking of the rows by the letters. This means that most mixing combination pairs have similar mean storage moduli. Therefore, the data associated with the first eight combinations can be "grouped" into one set of mean storage modulus data for the purpose of response surface modeling. This is designated by the group S1 in Table IV. The same is true for the last three combinations involving ultrasonication (group S3 in Table IV). The combination of oxidized VGCNF/dispersing agent/US (group S2 in Table IV) is the only combination differing significantly from the other combinations involving ultrasonication. Therefore, three separate response surfaces were generated for the data associated with the qualitative factor combinations (Table IV): (^{1}) grouped HS and HS/US (S1), (^{2}) oxidized VGCNF/dispersing agent/US (S2), and (^{3}) grouped US excluding S2 (S3). Hence, the 12 possible response surfaces were reduced to only three, simplifying data analysis and subsequent modeling. The predictions of one of these three response surfaces can be used for any desired combination of factor levels as long as that combination belongs to the group (Table IV).

A general cubic response surface model with two independent variables (X_1 and X_2) can be expressed as:

$$Y_i = \beta_0 + \sum_{i=1}^{2} \beta_i X_i + \sum_{i=1}^{2} \beta_{ii} X_i^2 + \beta_{12} X_1 X_2 + \\ + \sum_{i=1}^{2} \beta_{iii} X_i^3 + \beta_{112} X_1^2 X_2 + \beta_{122} X_1 X_2^2 + e_i, \quad (1)$$

where Y_i is the dependent variable, β_0 is the intercept, all the other β's are model parameters, and e_i is the model error term. Here, the VGCNF weight fraction ($X_1 = W$) and temperature ($X_2 = T$) were independent variables and the storage modulus ($Y_i = S$) was the dependent variable. Cubic equations were fitted to the mean storage modulus data through backward elimination.[54] The insignificant model terms were removed to further refine the model. This involved conducting partial *t*-tests for the parameters by comparing their *P*-values, which are associated with their calculated *t*-values. Those parameters with *P*-values greater than 0.05 were removed. However, based on the "hierarchy principle,"[54] the lower order terms, which are completely contained in significant higher order terms, were retained in the models.

These regression analysis results are summarized in Table V, where the model parameters, their estimates, their associated *t*- and *P*-values,[55] and R^2 and adjusted R^2 values are shown. Parameters with *P*-values less than $\alpha = 0.05$ were considered significant model terms. The *t*-values are given for reference purposes.

Based on the LSD multiple comparison results in Table IV and regression analyses in Table V, the three RSMs obtained are expressed as:

$$S_1 = 2231.2 + 2567.3W + 0.9T - 5025.9W^2 - 10.6WT \\ - 0.1T^2 + 2678.7W^3 - 0.07WT^2, \quad (2)$$

$$S_2 = 2398.4 + 1299.7W - 4.3T - 1341.1W^2 + 7.0WT \\ - 0.07T^2 + 8.1W^2T - 0.1WT^2, \quad (3)$$

$$S_3 = 2439.1 + 1384.0W - 4.3T - 1355.4W^2 - 4.1WT \\ - 0.07T^2 + 14.0W^2T - 0.08WT^2, \quad (4)$$

where S_i is the storage modulus (i = 1,2,3 representing the groups S1, S2, and S3 in Table IV), W is the VGCNF weight fraction, and T is the temperature. These models describe 97.8%, 99.6%, and 98.0% of the variations in the mean storage modulus for the S1, S2, and S3 data groups, respectively (Table V). Figure 2 shows a representative 3D response surface plot of the storage modulus versus temperature and VGCNF weight fraction for the group S1 (grouped HS and HS/US data). The response surfaces for the other data groups can be generated in the same fashion. The 3D surface in Figure 2 is color coded to indicate regions of high (red) and low storage modulus (blue). The contour plots are projected on the *W*-*T* plane to show the regions with constant storage modulus. Overall, the storage modulus (or proportionally Young's modulus) decreases with increasing temperature, which is a common feature of polymers. Furthermore, an overall increase in the storage

Table V. Regression Analyses for the Storage Modulus Data

Parameter	Degrees of freedom	Parameter estimate	Standard error	*t*-value	*P*-value
S1 (grouped high-shear mixing and coupled high-shear mixing/ultrasonication combinations) (R^2 = 0.978, adjusted R^2 = 0.977):					
β_0	1	2231.2	64.1	34.8	<0.0001
β_1	1	2567.3	180.2	14.3	<0.0001
β_2	1	0.9	1.9	0.5	0.6276
β_{11}	1	−5025.9	377.5	−13.3	<0.0001
β_{12}	1	10.6	3.2	3.4	0.0010
β_{22}	1	−0.1	0.01	−8.1	<0.0001
β_{111}	1	2678.7	48.1	10.8	<0.0001
β_{122}	1	−0.07	0.02	−3.5	0.0006
S2 (ultrasonication with oxidized VGCNF and dispersing agent combination) (R^2 = 0.996, adjusted R^2 = 0.994):					
β_0	1	2398.4	104.5	23.0	<0.0001
β_1	1	1299.7	292.8	4.4	0.0008
β_2	1	−4.3	3.1	−1.4	0.1848
β_{11}	1	−1341.1	243.0	−5.5	0.0001
β_{12}	1	7.0	5.8	1.2	0.2506
β_{22}	1	−0.07	0.02	−3.4	0.0051
β_{112}	1	8.1	3.0	2.7	0.0183
β_{122}	1	−0.11	0.03	−3.3	0.0060
S3 (grouped ultrasonication combinations excluding S2) (R^2 = 0.980, adjusted R^2 = 0.977):					
β_0	1	2439.1	127.8	19.1	<0.0001
β_1	1	1384.0	357.9	3.9	0.0003
β_2	1	−4.3	3.7	−1.2	0.2546
β_{11}	1	−1355.4	297.0	−4.6	<0.0001
β_{12}	1	−4.1	7.1	−0.6	0.5638
β_{22}	1	−0.07	0.02	−3.1	0.0034
β_{112}	1	14.0	3.6	3.9	0.0003
β_{122}	1	−0.08	0.04	−2.1	0.0416

modulus is observed for the VGCNF/VE nanocomposites compared to that of the neat VE. The latter result makes sense given the reinforcing (stiffening) effect of VGCNFs.

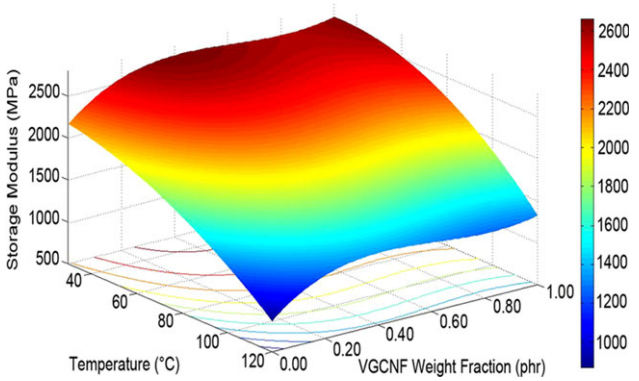

Figure 2. The predicted response surface and contour plots for the storage modulus as a function of VGCNF weight fraction and temperature for the S1 data group (grouped high-shear mixing and coupled high-shear mixing/ultrasonication combinations). [Color figure can be viewed in the online issue, which is available at wileyonlinelibrary.com.]

Two-dimensional (2D) graphs were generated from the eqs. (2)–(4) to better depict the predicted storage modulus as a function of VGCNF weight fraction and temperature. The predicted storage moduli for the S1 data group are plotted as a function of VGCNF weight fraction for different temperatures in Figure 3. For a given temperature, the predicted storage modulus increases with increasing amounts of VGCNFs up to a local maximum around $W \approx 0.40$ phr. This represents an increase of roughly 20% in the predicted storage modulus of nanocomposites at a given temperature compared to that of the neat VE ($W = 0.00$ phr). The predicted storage moduli remained relatively unchanged as the VGCNF weight fraction was further increased. This suggests that nanocomposites prepared with $W \approx 0.40$ phr of VGCNFs will maximize the storage modulus over the entire temperature range of study. A local maximum in the stiffness of polymer matrices with the addition of nanoreinforcements is often reported in the literature.[56,57] This phenomenon is for most part correlated to the level of nanoreinforcement dispersion in the matrix. Better nanoreinforcement dispersion translates into higher mechanical property improvement of the polymer nanocomposite.[46] At higher nanoreinforcement weight fractions, the dispersion becomes much

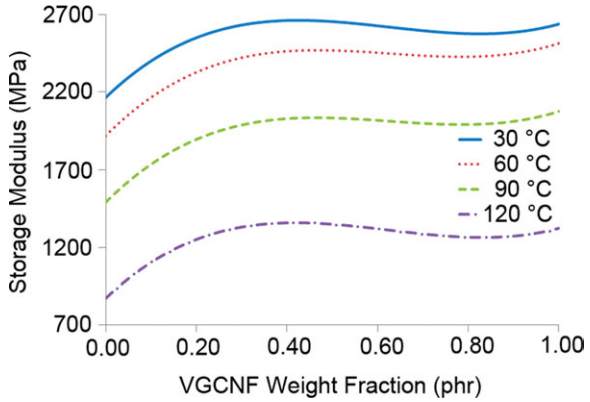

Figure 3. Predicted storage modulus as a function of VGCNF weight fraction for different temperatures. The data belongs to the S1 data group (grouped high-shear mixing and coupled high-shear mixing/ultrasonication combinations). [Color figure can be viewed in the online issue, which is available at wileyonlinelibrary.com.]

more difficult and the presence of nanoreinforcement agglomerates is more prevalent.

In Figure 4, a representative scanning electron micrograph of the fracture surface of a VGCNF/VE nanocomposite is shown. At a VGCNF weight fraction of 1.00 phr, a number of large-size nanofiber agglomerates can easily be located in the specimen. From a pragmatic point of view, the nanocomposites with lower VGCNF weight fractions will be less expensive, easier to process due to lower VGCNF/VE resin blend viscosity, and may exhibit higher strengths due to reduced numbers of large carbon nanofiber agglomerates than nanocomposites fabricated with higher VGCNF content. The optimal VGCNF amount ($W \approx 0.40$) that maximizes the predicted storage moduli over a range of temperatures can be compared to values from our previous room temperature study (0.37 phr for pristine VGCNFs and 0.54 phr for oxidized VGCNFs).[42] Similar to the results shown in Figure 2, the predicted storage moduli decrease as the temperature increases, which is the expected behavior for polymers. Similar plots can also be generated for the S2 and S3 data groups.

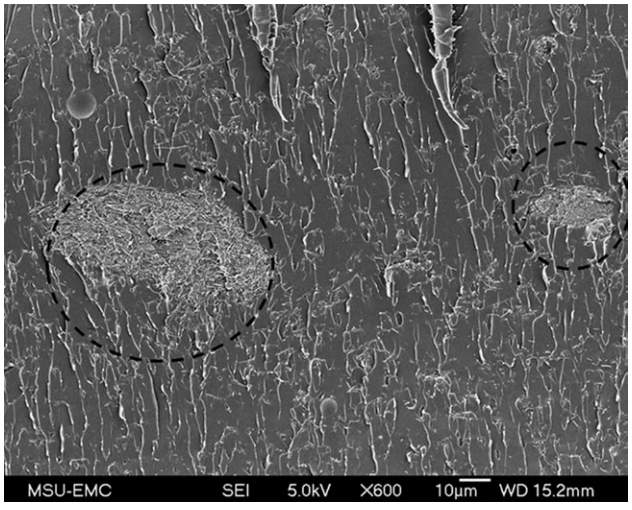

Figure 4. A representative scanning electron micrograph of the fracture surface of a VGCNF/VE nanocomposite specimen containing oxidized VGCNFs, dispersing agent, and a VGCNF weight fraction of 1.00 phr, prepared using coupled high-shear mixing/ultrasonication. Two nanofiber agglomerates, roughly 30 and 70 μm in size, are circled.

The LSD comparisons (Table IV) and the developed RSMs [eqs. (2–4)] illustrate that the S1 data group gives higher mean storage modulus values over the entire temperature range compared to the S2 and S3 data groups. This suggests that US does not increase the storage modulus of the nanocomposites to the same degree as HS or HS/US. Evidently, US is not as effective in dispersing VGCNFs in the VE matrix as the other two mixing techniques.

The predicted storage moduli are plotted in Figure 5 as a function of VGCNF weight fraction for the S1, S2, and S3 data groups (Table IV) at 30°C and 90°C. All three grouped data combinations exhibit nearly the same behavior at 30°C [Figure 5(a)]. This is consistent with the results obtained for the room temperature analysis,[42] where the storage modulus was independent of the mixing method. As the temperature increases [Figure 5(b)], the S1 data group gives markedly higher storage moduli over the entire VGCNF weight fraction range than do the S2 and S3 combinations. This highlights the effectiveness of high-shear mixing

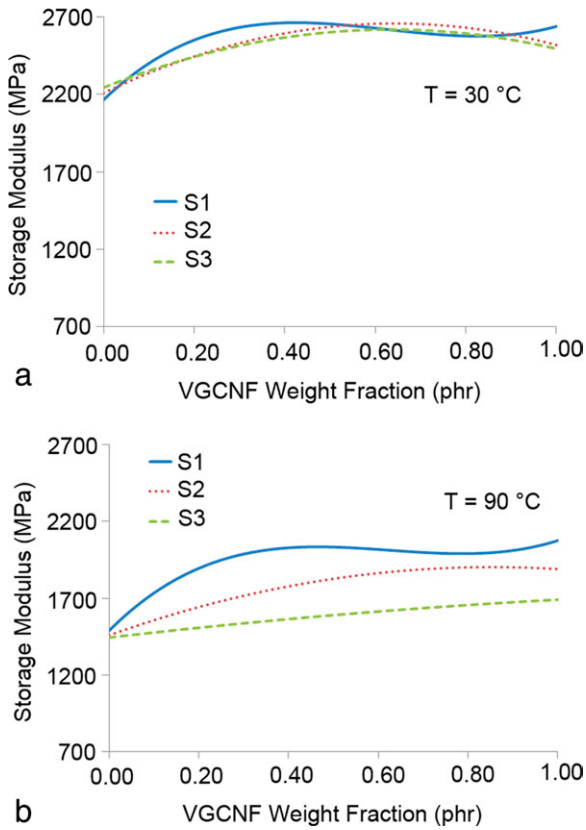

Figure 5. Comparisons between predicted storage moduli for the S1 (grouped high-shear mixing and coupled high-shear mixing/ultrasonication combinations), S2 (ultrasonication with oxidized VGCNF and dispersing agent combination), and S3 data groups (grouped ultrasonication combinations excluding S2) for temperatures (T) of (a) 30°C and (b) 90°C. [Color figure can be viewed in the online issue, which is available at wileyonlinelibrary.com.]

Table VI. Analysis of Variance (ANOVA) for the Loss Modulus Data

Source of variation	Degrees of freedom	Sum of squares	Mean square	*F*-Value	*P*-Value[a]
Model	141	477367.9	3385.6	49.3	<0.0001
A: VGCNF type	1	12.2	12.2	0.2	0.6751
B: Use of dispersing agent	1	32.3	32.3	0.5	0.4949
C: Mixing method	2	9460.1	4730.1	68.8	<0.0001
W: VGCNF weight fraction	4	4900.9	1225.2	17.8	<0.0001
T: Temperature	3	397789.1	132596.4	1928.9	<0.0001
A×*B*	1	22.8	22.8	0.3	0.5659
A×*C*	2	672.3	336.2	4.9	0.0095
A×*W*	4	455.8	114.0	1.7	0.1660
A×*T*	3	86.4	28.8	0.4	0.7400
B×*C*	2	67.6	33.8	0.5	0.6131
B×*W*	4	173.3	43.3	0.6	0.6421
B×*T*	3	563.6	187.9	2.7	0.0478
C×*W*	8	4117.8	514.7	7.5	<0.0001
C×*T*	6	12349.7	2058.3	29.9	<0.0001
W×*T*	12	35027.6	2919.0	42.5	<0.0001
A×*B*×*C*	2	736.6	368.3	5.4	0.0062
A×*B*×*W*	4	97.1	24.3	0.4	0.8414
A×*B*×*T*	3	75.6	25.2	0.4	0.7772
A×*C*×*W*	8	1738.5	217.3	3.2	0.0032
A×*C*×*T*	6	1037.4	172.9	2.5	0.0263
A×*W*×*T*	12	318.9	26.6	0.4	0.9655
B×*C*×*W*	8	269.9	33.7	0.5	0.8602
B×*C*×*T*	6	1445.3	240.9	3.5	0.0035
B×*W*×*T*	12	626.3	52.2	0.8	0.6902
C×*W*×*T*	24	5291.1	220.5	3.2	<0.0001
Error	98	6736.9	68.7435	-	-
Total (corrected)	239	484104.7	-	-	-
Other Model Statistics					
Mean: 90.8			R^2: 0.986		
Coefficient of variation: 9.1%			Standard deviation: 8.3		

Note: The underlined three-factor interactions are significant. The lower order significant interactions were not considered in the analysis, because they are all contained in higher order interactions.
[a]Values <0.05 are considered significant in the analysis.

in dispersing the VGCNFs in the VE matrix, resulting in improved material properties at higher service temperatures.

The RSMs for the S1, S2, and S3 data groups can be used to assess the effects of *quantitative* factors (*W* and *T*) on the predicted storage moduli. The LSD multiple comparisons in Table IV are used to determine the *qualitative* factor levels resulting in the optimal values for the storage moduli. On this basis, comparing the factor level combinations within the S1 data group in Table IV reveals that the effects of HS and HS/US mixing methods on the predicted storage moduli were not significantly different from each other. Therefore, the HS mixing alone is recommended for maximizing the storage modulus over the entire temperature range (30–120°C). This provides added benefits of fast and economical processing. Examining the HS combinations in Table IV reveals that oxidized VGCNFs in the absence of dispersing agent (factor level combination in row one of Table IV) or pristine VGCNFs in the presence of dispersing agent (factor level combination in row three of Table IV) may be used to maximize the storage modulus over a range of temperatures. VGCNF surface oxidation and use of the dispersing agent affect storage modulus in a similar way when specimens are prepared using HS mixing. The optimal combination of factors may additionally depend on how they affect other material properties such as strength.

Loss Moduli

The ANOVA[27] was used to analyze the loss modulus data before predictive RSMs were developed. A complete set of loss modulus data pertaining to different treatment combinations are given by Nouranian.[52] Since only one batch was prepared for

Table VII. Multiple Comparison Results for the Mean Loss Modulus Data Using Least Significant Difference (LSD) for the Interaction Between the VGCNF Type, Use of Dispersing Agent, and Mixing Method ($A \times B \times C$)

t-Grouping		Least squares mean values for the loss modulus data (MPa)	VGCNF type (A)	Use of dispersing agent (B)	Mixing method (C)	
	M[a]	102.15	Oxidized	No	US[b]	
	M					
	M	100.95	Pristine	Yes	US	
	M					L1
	M	97.75	Pristine	No	US	
	M					
	M	97.45	Oxidized	Yes	US	
	N	89.45	Oxidized	No	HS/US[c]	
	N					
O	N	89.05	Pristine	No	HS[d]	
O	N					
O	N	88.60	Oxidized	Yes	HS/US	
O	N					
O	N	87.60	Pristine	Yes	HS/US	
O	N					L2
O	N	86.50	Pristine	Yes	HS	
O	N					
O	N	85.80	Oxidized	Yes	HS	
O						
O	P	84.20	Pristine	No	HS/US	
	P					
	P	79.90	Oxidized	No	HS	

Each group of data, i.e., L1 and L2, results in one response surface.
[a]Least squares means with the same letters are not significantly different from each other.
[b]Ultrasonic mixing.
[c]Coupled high-shear and ultrasonic mixing.
[d]High-shear mixing.

each treatment combination, there was no experimental error associated with the loss modulus data. The four- and five-factor interactions were assumed to be negligible in constructing an error term for the ANOVA analysis. The ANOVA results are shown in Table VI, where factorial effects were analyzed using ordered *F*-tests[53] starting from the three-factor interactions. Five significant three-factor effects (underlined in Table VI) were isolated by comparing the actual *P*-values of the factorial effects to the level of significance $\alpha = 0.05$:

1. Interaction between the VGCNF type (A), the use of dispersing agent (B), and the mixing method (C), i.e., $A \times B \times C$;
2. Interaction between the VGCNF type (A), the mixing method (B), and the VGCNF weight fraction (W), i.e., $A \times C \times W$;
3. Interaction between the VGCNF type (A), the mixing method (C), and the temperature (T), i.e., $A \times C \times T$;
4. Interaction between the use of dispersing agent (B), the mixing method (C), and the temperature (T), i.e., $B \times C \times T$;
5. Interaction between the mixing method (C), the VGCNF weight fraction (W), and the temperature (T), i.e., $C \times W \times T$.

All of the significant two- and three-factor interactions involving factors A, B, C, W, and T were contained in significant higher order interactions with the exception of the two-factor interaction $B \times W$. This interaction was not significant (P-value $= 0.6421 > 0.05$), so the remaining two-factor interactions and main effects were not further analyzed. The $A \times B \times C$ qualitative factorial interaction was significant. This interaction was analyzed to reduce the total number of generated response surfaces. Furthermore, all of the other significant three-factor interactions involved the *quantitative* factors, i.e., VGCNF weight fraction (W) and temperature (T), which were considered in the response surfaces. As a result, Fisher's LSD multiple comparisons[28] were conducted on the mean data to identify the significant $A \times B \times C$ factor level combinations. These are shown in Table VII, where "VGCNF type/dispersing agent/mixing method" combinations can be compared with one another. The letters in the *t*-grouping column (M, N, O, and P) establish relationships between the pairs of mean data.

Table VIII. Regression Analysis for the Loss Modulus Data

Parameter	Degrees of freedom	Parameter estimate	Standard error	*t*-Value	*P*-Value
L1 (grouped ultrasonication combinations) ($R^2 = 0.913$, adjusted $R^2 = 0.903$):					
β_0	1	−49.3	24.4	−2.0	0.0465
β_1	1	220.1	36.2	6.1	<0.0001
β_2	1	5.3	1.2	4.5	<0.0001
β_{11}	1	−435.6	75.8	−5.8	<0.0001
β_2	1	−1.4	0.6	−2.3	0.0255
β_{22}	1	−0.07	0.02	−4.3	<0.0001
β_{111}	1	248.3	49.8	5.0	<0.0001
β_{122}	1	0.01	0.004	3.4	0.0013
β_{222}	1	0.0003	0.00007	4.5	<0.0001
L2 (grouped high-shear mixing and coupled high-shear mixing/ultrasonication combinations) ($R^2 = 0.944$, adjusted $R^2 = 0.941$):					
β_0	1	11.8	17.1	0.7	0.4899
β_1	1	−73.2	25.9	−2.8	0.0053
β_2	1	2.7	0.8	3.3	0.0011
β_{11}	1	118.3	21.5	5.5	<0.0001
β_{12}	1	−0.6	0.5	−1.1	0.2567
β_{22}	1	−0.04	0.01	−3.8	0.0002
β_{112}	1	−1.8	0.3	−6.8	<0.0001
β_{122}	1	0.02	0.003	7.0	<0.0001
β_{222}	1	0.0002	0.00005	4.7	<0.0001

All four factor level combinations involving US alone gave the most consistently high mean loss moduli (the first four factor level combinations in Table VII). The last eight HS and HS/US combinations are chained in the *t*-grouping column. Thus, all 12 combinations were grouped into two sets of mean loss modulus data for use in response surface modeling. One set is for specimens prepared using US (designated as L1) and the second is for specimens prepared using HS and HS/US (L2). The predictions for both of these response surfaces can be used for any combination of factor levels. The only requirement is that the combination belongs to the associated group (Table VII).

Cubic equations were fitted to the mean loss modulus data and two RSMs were generated:

$$L_1 = -49.3 + 220.1W + 5.3T - 435.6W^2 - 1.4WT - 0.07T^2 + +248.3W^3 + 0.01WT^2 + 0.0003T^3, \quad (5)$$

$$L_2 = 11.8 - 73.2W + 2.7T + 118.3W^2 - 0.6WT - 0.04T^2 - -1.8W^2T + 0.02WT^2 + 0.0002T^3, \quad (6)$$

where VGCNF weight fraction (W) and temperature (T) are independent variables and the loss modulus ($L_{i,\ i\ =\ 1,2}$) is the dependent variable. Equations (5) and (6) pertain to L1 and L2 data groups (Table VII), respectively, where the insignificant model terms in the original cubic equations were removed through backward elimination invoking the hierarchy principle.[54] The regression analysis results are given in Table VIII, where β_0 is the intercept, and the other β's are model parameters [see eq. (1)]. Parameters with *P*-values of less than $\alpha = 0.05$ are considered significant model terms.

The two RSMs [eqs. (5) and (6)] describe 91.3% and 94.4% of the variations in the mean loss modulus data for the L1 and L2 data groups (Table VII), respectively. Both response surfaces are plotted in Figure 6, where regions of constant loss moduli are projected onto the *W*-*T* plane. As can be seen in Figure 6(a,b), the predicted loss moduli are a complex function of VGCNF weight fraction and temperature. 2D graphs (Figures 7 and 8) are used to assess the effects of VGCNF weight fraction and temperature on the predicted loss moduli for the L1 and L2 data groups, respectively.

All nanocomposites pertaining to the US data combination grouping (L1) gave equal or higher loss moduli than the neat VE ($W = 0.00$ phr) at all temperatures from 30°C to 120°C [Figure 7(a)]. The predicted loss modulus increased with increasing amounts of VGCNFs up to a local maximum occurring at $W \approx 0.25$ phr [Figure 7(a)]. Beyond this point, the loss moduli decreased slightly or leveled off at higher VGCNF weight fractions. The increase in loss moduli at lower VGCNF weight fractions ($W < 0.25$ phr) may be primarily due to interfacial slip occurring between the individual nanofibers and the matrix, frictional sliding between entangled and interlocked VGCNFs contained in agglomerates, and other dissipative mechanisms.[50] Ultrasonication can result in poor nanofiber dispersion and increased numbers of nanofiber agglomerates.[42] At higher VGCNF weight fractions ($W > 0.50$ phr), the loss moduli tended to decrease somewhat at lower temperatures. This may be due to markedly reduced nanocomposite ductility

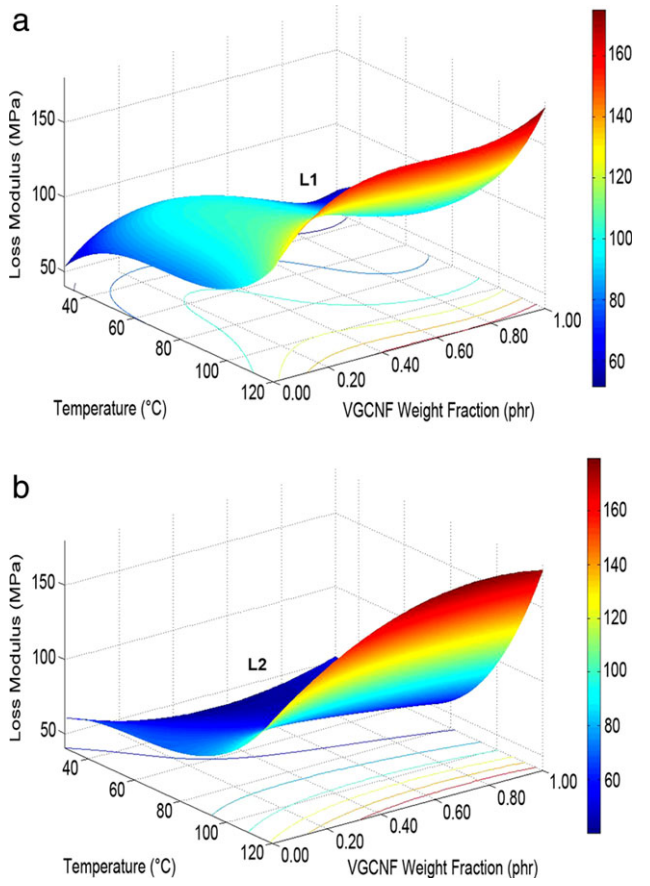

Figure 6. The predicted response surface and contour plots for the loss modulus as a function of VGCNF weight fraction and temperature for (a) the L1 data group (grouped ultrasonication combinations) and (b) the L2 data group (grouped high-shear mixing and coupled high-shear mixing/ultrasonication combinations). [Color figure can be viewed in the online issue, which is available at wileyonlinelibrary.com.]

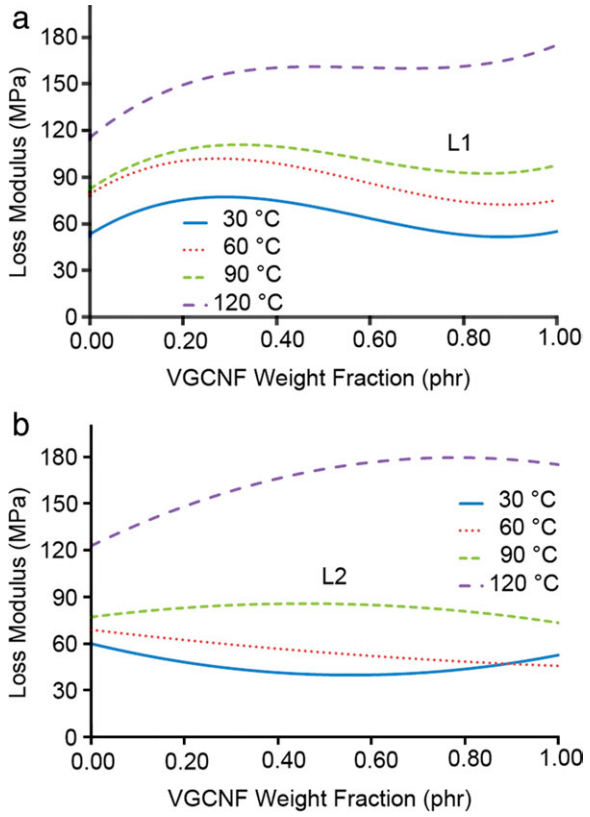

Figure 7. Predicted loss modulus as a function of VGCNF weight fraction for different temperatures for (a) the L1 data group (grouped ultrasonication combinations) and (b) the L2 data group (grouped high-shear mixing and coupled high-shear mixing/ultrasonication combinations). [Color figure can be viewed in the online issue, which is available at wileyonlinelibrary.com.]

resulting from increased VGCNF content. Conversely, the slight increase in the loss modulus with increasing amounts of VGCNFs at 120°C is likely attributable to changes in the VE matrix ductility at elevated temperatures.

In contrast to the L1 group of specimens (US data combination grouping), all VGCNF weight fractions for L2 specimens (HS data combination grouping) exhibited predicted loss moduli values that were lower than the neat VE at temperatures below ~90°C [Figure 7(b)]. This makes sense since HS or HS/US yields better nanofiber dispersion, reduced numbers and sizes of nanofiber agglomerates, and potentially less interfiber frictional slipping. At higher temperatures, the predicted loss moduli for all nanocomposites exceed those of the neat VE [Figure 7(b)]. In general, the higher the VGCNF weight fraction, the lower the predicted loss modulus, except at elevated temperatures where the energy dissipation is more matrix dominated. VGCNFs tend to reduce nanocomposite ductility, especially for specimens containing well-dispersed nanofibers at lower temperatures where the matrix is less ductile [Figure 7(b)].

In Figure 8, the predicted loss moduli are plotted as functions of VGCNF weight fraction for different data groups (L1 and L2) at temperatures of 30°C and 120°C. Specimens prepared using US combinations alone (L1) had higher loss moduli than the specimens prepared using HS and HS/US combinations

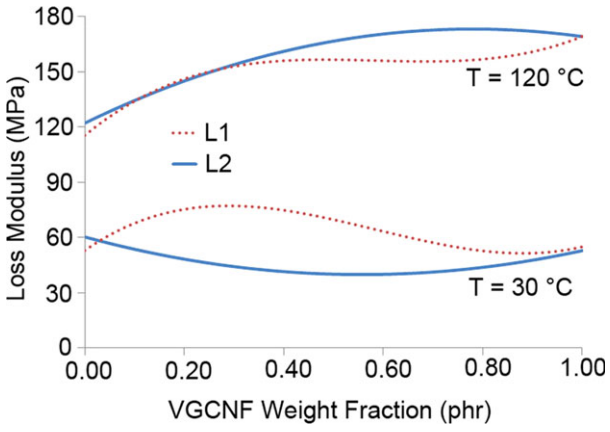

Figure 8. Comparisons between predicted loss modulus of the L1 (grouped ultrasonication combinations) and L2 data groups (grouped high-shear mixing and coupled high-shear mixing/ultrasonication combinations) at temperatures (T) of 30°C and 120°C. [Color figure can be viewed in the online issue, which is available at wileyonlinelibrary.com.]

(L2) at the low temperature. However, at 120°C, the specimens prepared using both data groups demonstrated marked increases in loss moduli. A comparison of Figures 7 and 8 shows that the loss moduli are far more sensitive to variations in temperature than to changes in the VGCNF weight fraction or mixing method. These results underscore the matrix-dominated behavior at elevated temperatures.

Consistent with the approach used to assess the storage modulus, Table VII may be used to select *qualitative* factor levels leading to the desired loss modulus. For example, a combination of oxidized VGCNFs, no dispersing agent, and US (factor level combination in row one of Table VII) may be used to maximize the loss modulus. Such insights would not have been possible when employing more traditional *ad hoc* or *one-at-a-time* experimental strategies. To further validate the RSMs, nanocomposite storage and loss moduli were calculated at the intermediate temperature of 70°C. The predicted storage modulus (2114 MPa) for a nanocomposite containing 0.50 phr oxidized VGCNFs (plus dispersing agent) prepared using high-shear mixing fell within 5.6% of the experimentally measured value (2240 MPa). Similarly, the predicted loss modulus (101 MPa) for a nanocomposite containing 0.25 phr oxidized VGCNFs (no dispersing agent) prepared with ultrasonication was within 1% of the measured value (100 MPa). Based upon the RSM, the latter combination of formulation and processing factors will maximize the loss modulus.

As an aside, the damping coefficient tan δ (i.e., ratio of loss modulus to storage modulus) may also be treated as a separate response or simply evaluated using eqs. (2)–(6). The tan δ function provides valuable information regarding the dynamic properties, dissipation, and glass transition temperature (T_g) of the polymer nanocomposite. These results underscore the utility of RSMs in determining the combination of formulation and processing parameters leading to optimal nanocomposite properties over a range of operating conditions.

SUMMARY AND CONCLUSIONS

A designed experimental study investigated the effects of formulation and processing factors (including temperature) on the storage and loss moduli of vapor-grown carbon nanofiber (VGCNF)/vinyl ester (VE) nanocomposites. Response surface models were developed and used to predict nanocomposite storage and loss moduli as a function of five independent factors: (1) VGCNF type, (2) use of dispersing agent, (3) mixing method, (4) VGCNF weight fraction, and (5) temperature.

To maximize the storage modulus over the entire 30–120°C temperature range, specimens should be prepared using *high-shear mixing* and a VGCNF weight fraction of ~0.40 phr. Furthermore, use of either oxidized VGCNFs or pristine VGCNFs with dispersing agent will lead to similar improvements in storage moduli. Similarly, to maximize the loss modulus, nanocomposites should be fabricated using ~0.25 phr of oxidized VGCNFs and *ultrasonication*.

The current study demonstrates the use of statistical design of experiments to explore complex interactions between formulation and processing factors affecting the viscoelastic behavior of polymer nanocomposites. Such interactions cannot be assessed in traditional one-factor experimental studies. The results of the statistical analyses can be used to establish factor levels leading to optimal material behavior. The response surface models developed in this study may be used to tailor the viscoelastic properties of VGCNF/VE nanocomposites over a wide range of service environments.

ACKNOWLEDGMENTS

This work was sponsored by the U. S. Department of Energy under contract DE-FC26-06NT42755. Special thanks go to William Joost, Department of Energy's technology area development manager.

REFERENCES

1. Rangari, V. In Advances in Nanocomposites—Synthesis, Characterization and Industrial Applications; Reddy, B., Ed.; InTech Open Access Publisher, **2011**. Available at: http://www.intechopen.com/books/advances-in-nanocomposites-synthesis-characterization-and-industrial-applications.
2. Hussain, F.; Hojjati, M.; Okamoto, M.; Gorga, R. E. *J. Compos. Mater.* **2006**, *40*, 1511.
3. United States Air Force Materials Research Highlights, Materials and Manufacturing Directorate, Air Force Research Laboratory. Shape Memory Polymer Materials Improve Composite Surface Antenna Reflectors; United States Air Force Materials Research Highlights, Materials and Manufacturing Directorate, Air Force Research Laboratory: Dayton, OH, **2010**.
4. Kotsilkova, R.; Pissis, P. Thermoset Nanocomposites for Engineering Applications; Smithers Rapra Technology: Shropshire, UK, **2007**.
5. Thostenson, E. T.; Li, C.; Chou, T. W. *Compos. Sci. Technol.* **2005**, *65*, 491.
6. Tibbetts, G. G.; Lake, M. L.; Strong, K. L.; Rice, B. P. *Compos. Sci. Technol.* **2007**, *67*, 1709.
7. Elgafy, A.; Lafdi, K. *Carbon* **2005**, *43*, 3067.
8. Kumar, S.; Rath, T.; Mahaling, R.; Reddy, C.; Das, C.; Pandey, K.; Srivastava, R.; Yadaw, S. *Mater. Sci. Eng. B* **2007**, *141*, 61.
9. Agarwal, S.; Khan, M. M. K.; Gupta, R. K. *Polym. Eng. Sci.* **2008**, *48*, 2474.
10. Moore, A. L.; Cummings, A. T.; Jensen, J. M.; Shi, L.; Koo, J. H. *J. Heat Transfer* **2009**, *131*, 091602–5.
11. Yang, S.; Benitez, R.; Fuentes, A.; Lozano, K. *Compos. Sci. Technol.* **2007**, *67*, 1159.
12. Wu, S.-H.; Natsuki, T.; Kurashiki, K.; Ni, Q.-Q.; Iwamoto, M.; Fujii, Y. *Adv. Compos. Mater.* **2007**, *16*, 195.
13. Allaoui, A.; Hoa, S. V.; Pugh, M. D. *Compos. Sci. Technol.* **2008**, *68*, 410.
14. Al-Saleh, M. H.; Sundararaj, U. *Carbon* **2009**, *47*, 2.
15. Yang, Y.; Gupta, M. C.; Dudley, K. L. *Nanotechnology* **2007**, *18*, 345701.
16. Nanni, F.; Travaglia, P.; Valentini, M. *Compos. Sci. Technol.* **2009**, *69*, 485.
17. Al-Saleh, M. H.; Sundararaj, U. *Polymer* **2010**, *51*, 2740.

18. Zhongfu, Z.; Jan, G. *Sci. Technol. Adv. Mater.* **2009**, *10*, 015005.
19. Lakshminarayanan, P. V.; Toghiani, H.; Pittman, C. U., Jr. *Carbon* **2004**, *42*, 2433.
20. Li, J.; Vergne, M. J.; Mowles, E. D.; Zhong, W. H.; Hercules, D. M.; Lukehart, C. M. *Carbon* **2005**, *43*, 2883.
21. Rasheed, A.; Dadmun, M. D.; Britt, P. F. *J. Polym. Sci. Part B: Polym. Phys.* **2006**, *44*, 3053.
22. Sadeghian, R.; Gangireddy, S.; Minaie, B.; Hsiao, K.-T. *Compos. Part A: Appl. Sci. Manuf.* **2006**, *37*, 1787.
23. Tibbetts, G. G.; McHugh1, J. J. *J. Mater. Res.* **1999**, *14*, 2871.
24. Patton, R.; Pittman, C.; Wang, L.; Hill, J.; Day, A. *Compos. Part A: Appl. Sci. Manuf.* **2002**, *33*, 243.
25. Jimenez, G. A.; Jana, S. C. *Compos. Part A: Appl. Sci. Manuf.* **2007**, *38*, 983.
26. Faraz, M. I.; Bhowmik, S.; De Ruijter, C.; Laoutid, F.; Benedictus, R.; Dubois, P.; Page, J. V. S.; Jeson, S. *J. Appl. Polym. Sci.* **2010**, *117*, 2159.
27. Montgomery, D. C. Design and Analysis of Experiments; John Wiley & Sons: Hoboken, NJ, **2009**.
28. Myers, R. H.; Montgomery, D. C.; Anderson-Cook, C. M. Response Surface Methodology: Process and Product Optimization Using Designed Experiments; John Wiley & Sons: Hoboken, NJ, **2009**.
29. Ilzarbe, L.; Álvarez, M. J.; Viles, E.; Tanco, M. *Qual. Reliab. Eng. Int.* **2008**, *24*, 417.
30. Lacy, T. E.; Samarah, I. K.; Tomblin, J. S. *SAE Int. J. Aerosp.* **2002**, 126.
31. Samarah, I. K.; Weheba, G. S.; Lacy, T. E. *SAE Int. J. Aerosp.* **2006**, 767.
32. Samarah, I. K.; Weheba, G. S.; Lacy, T. E. *J. Appl. Stat.* **2006**, *33*, 429.
33. Yong, V.; Hahn, H. T. *Nanotechnology* **2005**, *16*, 354.
34. Nouranian, S.; Garmabi, H.; Mohammadi, N. *J. Adhes. Sci. Technol.* **2007**, *21*, 705.
35. Chow, W.; Yap, Y. *Express. Polym. Lett.* **2008**, *2*, 2.
36. Joulazadeh, M.; Navarchian, A. H. *Polym. Adv. Technol.* **2010**, *21*, 263.
37. Majdzadeh-Ardakani, K.; Navarchian, A. H.; Sadeghi, F. *Carbohydr. Polym.* **2010**, *79*, 547.
38. Khosrokhavar, R.; Naderi, G.; Bakhshandeh, G. R.; Ghoreishy, M. H. R. *Iran Polym. J.* **2011**, *20*, 41.
39. Plaseied, A.; Fatemi, A.; Coleman, M. R. *Polym. Polym. Compos.* **2008**, *16*, 405.
40. Torres, G. W.; Nouranian, S.; Lacy, T. E.; Toghiani, H.; Pittman, C. U., Jr.; Dubien, J. *J. Appl. Polym. Sci., to appear.*
41. Hutchins, J. W.; Sisti, J.; Lacy, T. E., Jr.; Nouranian, S.; Toghiani, H.; Pittman, C. U., Jr. 50th AIAA/ASME/ASCE/AHS/ASC Structures, Structural Dynamics and Materials Conference, Palm Springs, CA, 2009.
42. Nouranian, S.; Toghiani, H.; Lacy, T. E.; Pittman, C. U.; Dubien, J. *J. Compos. Mater.* **2011**, *45*, 1647.
43. Yoon, P.; Fornes, T.; Paul, D. *Polymer* **2002**, *43*, 6727.
44. Ellis, T. S.; D'Angelo, J. S. *J. Appl. Polym. Sci.* **2003**, *90*, 1639.
45. Ash, B. J.; Siegel, R. W.; Schadler, L. S. *J. Polym. Sci. Part B: Polym. Phys.* **2004**, *42*, 4371.
46. Yasmin, A.; Luo, J.; Abot, J.; Daniel, I. *Compos. Sci. Technol.* **2006**, *66*, 2415.
47. Li, T. C.; Ma, J.; Wang, M.; Tjiu, W. C.; Liu, T.; Huang, W. *J. Appl. Polym. Sci.* **2007**, *103*, 1191.
48. Menard, K. P. Dynamic Mechanical Analysis: A Practical Introduction; CRC Press: Boca Raton, FL, **2008**.
49. Buravalla, V. R.; Remillat, C.; Rongong, J. A.; Tomlinson, G. R. *Smart Mater. Bull.* **2001**, *2001*, 10.
50. Sun, L.; Gibson, R. F.; Gordaninejad, F.; Suhr, J. *Compos. Sci. Technol.* **2009**, *69*, 2392.
51. Li, X.; Gao, H.; Scrivens, W. A.; Fei, D.; Xu, X.; Sutton, M. A.; Reynolds, A. P.; Myrick, M. L. *Nanotechnology* **2004**, *15*, 1416.
52. Nouranian, S. Vapor-Grown Carbon Nanofiber/Vinyl Ester Nanocomposites: Designed Experimental Study of Mechanical Properties and Molecular Dynamics Simulations; Ph.D. Dissertation. Mississippi State University: Mississippi State, MS, **2011**.
53. Ellison, S. L. R.; Barwick, V.; Farrant, T. J. Practical Statistics for the Analytical Scientist: A Bench Guide; The Royal Society of Chemistry Publishing: Cambridge, UK, **2009**.
54. Kleinbaum, D. G.; Klein, M.; Pryor, E. R. Logistic Regression: A Self Learning Text; Springer: New York, NY, **2010**.
55. Ott, L.; Longnecker, M. *An Introduction to Statistical Methods and Data Analysis*; Brooks/Cole Cengage Learning: Belmont, CA, **2008**.
56. Jordan, J.; Jacob, K. I.; Tannenbaum, R.; Sharaf, M. A.; Jasiuk, I. *Mater. Sci. Eng. A* **2005**, *393*, 1.
57. Kanny, K.; Moodley, V. *J. Eng. Mater. Technol.* **2007**, *129*, 105.